



African Journal of Biological Sciences



MATHEMATICAL MODELS TO DESCRIBE THE DRYING KINETICS OF *SARCOCEPHALUS LATIFOLIUS* BARK

AUTHORS:

Dorcas Sola^{1*}, Max Seke Vangu^{2,5}, Altesse Benge Kade³, Bienvenu Mvingu Kamaluanda⁴, Blaise Mbala Mavinga⁴, Albert Lundemba Singa⁴ & Louis Efoto Eale²

AFFILIATIONS:

¹ Life Sciences Department / University of Kinshasa

² Physics & Technology Department / University of Kinshasa

³ Faculty of Petroleum, Gas, and New Energies / University of Kinshasa

⁴ Chemistry Department / University of Kinshasa

⁵ CoE-CBRN / DRC

MAILS & ORCID

| | |
|-----------------------------|---|
| Dorcas Sola Tabitha: | 0009-0008-8099-6456: dorcassola295@gmail.com / +243822307290 |
| Max Seke Vangu: | 0009-0007-4886-1132: max.seke@unikin.ac.cd |
| Altesse Benge kade : | 0009-0009-6292-6451 : altesse.benge@unikin.ac.cd |
| Blaise Mbala Mavinga: | 0000-0001-8020-6700: blaise.mbala@unikin.ac.cd |
| Bienvenu Mvingu Kamalandua: | 0000-0003-4031-9510: bienvenu.mvingu@unikin.ac.cd |
| Albert Lundemba Singa : | 0000-0002-7890-2368: albert.lundemba@unikin.ac.cd |
| Louis Efoto Eale: | 0000-0003-4979-123X: louis.efoto@unikin.ac.cd |

ABSTRACT

The drying kinetics of *Sarcocephalus Latifolius* bark, collected in Mbanza-Ngungu, Democratic Republic of the Congo, in central Kongo, were investigated employing various mathematical models including Page, Logarithmic, Two Terms, Verna et al., Midili, Peleg, and Logistic. The bark, precut and fractionated into sizes ranging from 0.5cm to 10cm, underwent drying in open air. Humidity levels were monitored closely, as excessive moisture encourages toxin proliferation, rendering the species unfit for consumption.

The models were validated using statistical parameters such as RMSE, RSE, and R^2 via Matlab with the Curve Fitting Tools library. Detailed analysis revealed that smaller bark sizes exhibited optimal drying times, with the logistic and logarithmic models displaying higher optima.

Additionally, a powder XRD analysis unveiled a notable presence of alkali sulfates, commonly utilized in water purification and corrosion prevention. The results indicate the Page model as the most suitable for describing the bark drying process, exhibiting minimal prediction errors. Nevertheless, the logistic and logarithmic models also yielded favorable outcomes. These findings advocate for the exploration of *Sarcocephalus Latifolius* bark for novel applications and technological advancements.

Keywords: Mathematical models, Drying kinetics, *Sarcocephalus Latifolius*, Bark composition, Moisture content, Phytochemical screening and Medicinal plant

RÉSUMÉ

La cinétique de séchage de l'écorce de *Sarcocephalus Latifolius*, récoltée à Mbanza-Ngungu, en République démocratique du Congo, au Kongo central est suivie. Divers modèles mathématiques, dont ceux de Page, Logarithmique, Two Terms, Verna et al., Midili, Peleg, et Logistique, ont été utilisés. Préalablement coupée et fractionnée en tranches de 0,5 cm à 10 cm, l'écorce a subi un processus de séchage à l'air libre. Le monitoring du taux d'humidité était observé, du fait que son excès favorise la propagation de toxines compromettant la qualité des échantillons.

Les paramètres statistiques tels que RMSE, RSE et R^2 , via Matlab avec la bibliothèque Curve Fitting Tools ont permis la validation des modèles. L'analyse des différentes tailles d'écorce a révélé des temps de séchage optimaux pour les tranches les plus petites, avec des résultats supérieurs pour les modèles logistique et logarithmique.

Une analyse XRD de poudre a mis en évidence une présence de sulfates alcalins, souvent utilisés dans la purification de l'eau et la prévention de la corrosion des métaux. Les conclusions mettent en avant le modèle de Page comme le plus adéquat pour décrire ce processus de séchage, présentant une marge d'erreur minimale. Néanmoins, les modèles logistique et logarithmique ont également fourni des résultats satisfaisants, encourageant ainsi l'exploration de nouvelles applications et le développement de technologies innovantes basées sur les écorces de *Sarcocephalus Latifolius*.

Mots clés : Modèles mathématiques, *Sarcocephalus Latifolius*, Cinétique de séchage, Composition de l'écorce, Teneur en humidité, Screening Phytochimique et plante médicinale

I. INTRODUCTION

Natural substances, mainly of plant origin, play a important role in a multitude of fields, ranging from traditional medicine to the food industry. Among these valuable resources, plant barks stand out due to their numerous medicinal and nutritional applications. However, their quality and safety can be compromised if not properly processed, especially during the drying process.

Natural substances, mainly of plant origin, play a crucial role in a multitude of fields, ranging from traditional medicine to the food industry. Among these valuable resources, plant barks stand out due to their numerous medicinal and nutritional applications. However, their quality

and safety can be compromised if not properly processed, especially during the drying process.

In the Democratic Republic of Congo (DRC), biodiversity is rich and utilized in various fields such as medicine, biology, and agro-food industries. However, the plants used undergo alterations due to their water content, which can compromise their quality.

In the context of our study based on the barks of *Sarcocephalus Latifolius*, a plant used for centuries in various cultures for its medicinal properties, deserve special attention. The characteristics of this shrub, including its height of approximately 4 to 5 meters, its twisted trunk reaching up to 30 cm in diameter, as well as its spread-out and open canopy with intermingled flexible branches, have been described (Kaboré, 2015). This species, belonging to the Rutaceae family, exhibits two types of growth habits, namely arborescent and acaulescent, and has broadly elliptical or suborbicular leaves, flowers grouped in spherical inflorescences, and fruits with irregularly globose berries (Kaboré, 2015; Méa et al., 2021; Plassart, 2019; Traore, 2020; Badiaga et al., 2011).

Drying is essentially defined as the reduction of water content in plants, aiming to inhibit enzymatic and microbial activity, thus preserving the product to extend its shelf life (El Mtiai, 2023).

In the absence of adequate drying, these barks can present various problems that impact their quality and safety. Excessive moisture can promote the proliferation of molds and fungi, potentially producing toxins harmful to health. Likewise, there is a risk of undesirable fermentation, thereby altering the taste, odor, and texture of the barks, making them unfit for consumption. Moreover, inadequate drying of these barks can lead to a loss of active principles and essential bioactive compounds, thereby reducing the therapeutic or medicinal efficacy of the barks.

Lastly, poorly dried barks can develop unpleasant aromas and flavors due to the proliferation of undesirable microorganisms, rendering the product unappealing for consumption (El Mtiai, 2023).

Thus, a specific study on the drying kinetics concerning different sizes of *Sarcocephalus Latifolius* barks could provide crucial information to optimize this process and preserve the valuable medicinal and nutritional properties of this plant resource.

This study aims to experiment with the drying process of *Sarcocephalus Latifolius* barks according to their size to ensure the quality of the products at different stages of production. To achieve this, we apply various empirical mathematical models such as Page, Newton, Two Terms, Midilli, Ademiluyi, Peleg, Wang and Sing, Verna et al., Henderson and Pabis, as well

as Logistic and Logarithmic models, to characterize the drying kinetics. We also conduct a visual analysis of the obtained data using Matlab/Simulink. This integrated approach, combining theory and practice, aims to optimize the drying process and maximize the quality of the products at different stages of their transformation.

II. MATERIALS

II.1. BIOLOGICAL MATERIAL

The bark of *Sarcocephalus latifolius*, sourced from Mbanza-Ngungu in the Kongo Central, is the subject of this study. [Figure 1](#) indicates the location of the harvest, which was carried out in February 2020 in Mbanza-Ngungu, Kongo Central.

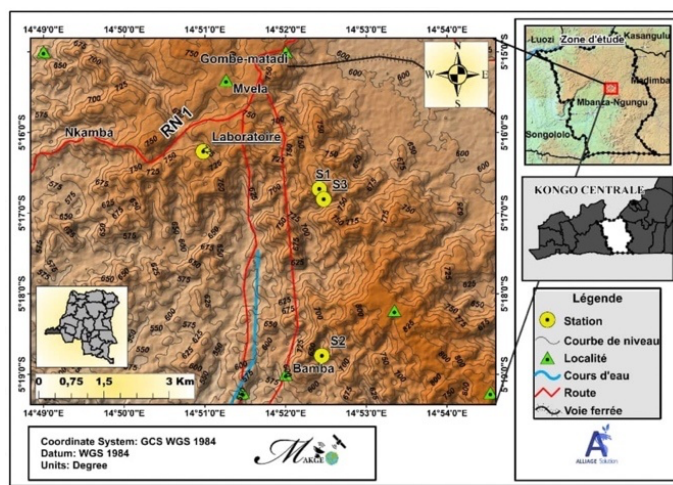


Figure 1: Map of the Harvest Site with Stations.

Also known as *Nauclea latifolia*, this plant is widely used in African traditional medicine, particularly for the treatment of malaria ([Sourabie et al., 2013](#)), diarrhea, typhoid fever, and other infections ([Ishimwe, 1983](#)). Its various parts are utilized in the form of decoctions and infusions, either alone or in combination with other medicinal plants ([Oise et al., 2014; Carlos et al., 2019; Togola et al., 2023; ME et al., 2016](#)). Extracts of *Sarcocephalus latifolius* are also known for their effectiveness as anthelmintic agents ([Diarra et al., 2015; Nurudeen et al., 2022](#)). This plant, used by the Bakongo tribes in northern Angola and Nigeria, is also cited as a commonly used remedy for HIV/AIDS management in Uganda ([Okhale et al., 2023; Kuete & Seukep, 2023; Kanteh & Noman, 2015; Masters et al., 2023](#)).

II.2. OTHER MATERIALS

The various instruments that enabled us to carry out this work are as follows:

- An Ohaus PioneerTM Precision balance.

The Ohaus PioneerTM Precision balance, depicted in [Figure 2a](#), is a precise and reliable weighing equipment, ideal for use in various fields such as research, pharmacy, and culinary applications. Featuring a robust platform and an easy-to-read LCD screen, it provides high accuracy and convenient functionalities such as automatic taring. This equipment is widely appreciated for its reliability and durability.



[Figure 2: a\) Ohaus PioneerTM Precision balance; b\) Saw used for sectioning plant organs.](#)

In the laboratory, the saw ([Figure 2b](#)) is used to cut them into pieces of appropriate size. These pieces are then utilized for scientific analyses and studies.

- A ruler, a saw, a knife, a pen, a notebook, and a Garmin GPS device, and a machete: These materials are essential for plant studies:

A ruler for precise measurements, a pen and notebook for recording observations, a Garmin GPS device for locating study sites and a machete for accessing challenging areas.

III. METHODOLOGY

- Drying:

After field collection, the samples were received, and sectioning into different sizes ranging from 0.5cm to 10cm was performed followed by drying in the laboratory at room temperature to continue the loss of water mass. The barks were spread out in laboratory B17 to air dry at room temperature, to continue the drying dynamics. During the drying process, mass samples were taken every 3 hours using a balance until the weight became constant.

- Phytochemical Screening:

Our research involves conducting screening to non-exhaustively evaluate a diversity of chemical compounds present in *Sarcocephalus* barks, focusing particularly on secondary metabolites such as alkaloids, flavonoids, triterpenes, phenols, steroids, saponins, free quinones, and polyphenols, as well as tannins, among others. Methanol and dichloromethane, used in this work, selectively interact with certain metabolites due to their chemical properties and polarity. Methanol, as a polar solvent, facilitates the extraction of electrically charged compounds such as polyphenols, flavonoids, alkaloids, phenolic acids, and tannins. Conversely, dichloromethane, an apolar solvent, is preferred for extracting neutrally charged

metabolites such as lipids, steroids, carbohydrates, and amino acids. Thus, solvent choice is crucial for obtaining efficient extraction of targeted metabolites.

- X-ray Analysis:

X-rays, as high-energy electromagnetic waves, interact with matter in various ways. The primary interaction involves atom ionization, inducing the emission of X-rays specific to each element, called X-ray fluorescence, used in chemical spectrometry. Another major interaction is X-ray diffraction by crystal planes, revealing the crystalline phases present in a sample via a diffractometer. For the analysis of *Sarcocephalus* substrate soil, the X-ray fluorescence spectrometer (XRF) was used, while the X-ray diffractometer (XRD) was applied for the analysis of *Sarcocephalus* powders. These instruments are from the Bruker brand and are depicted in [Figure 3](#). X-ray diffraction analysis (XRD)



Figure 3: (From left to right) D-2 diffractometer and S8-Tiger spectrometer from Bruker (Boulle, 2017)

Empirical Models & Drying Data Processing ([Moura et al., 2023](#); [Diógenes et al., 2022](#); [Page, 1949](#); [Paiva et al., 2023](#); [Midilli et al., 2002](#); [Verna et al., 1985](#))

| | |
|------------------|--|
| 1. Page | $MR = \exp(-k_0 * t^n)$ |
| 2. Midilli | $MR = A_0 * \exp(-k_0 * t^n) + A_1 * t$ |
| 3. Logarithmic | $MR = A_0 * \exp(-k_0 * t) + A_1$ |
| 4. Two-term | $MR = A_0 * \exp(-k_0 * t) + A_1 * \exp(-k_1 * t)$ |
| 5. Verna and al, | $MR = A_0 * \exp(-k_0 * t) + (1 - A_1) * \exp(-k_1 * t)$ |
| 6. Peleg | $MR = 1 + t / (A_0 + A_1 * t)$ |
| 7. Logistic | $MR = A_0 / (1 + A_1 * \exp(K_0 * t))$ |

The quantitative evaluation of model performance is conducted using MATLAB software to provide key statistical parameters. For each model, the software calculates the coefficient of determination (R^2) and adjusted R-squared (Adj- R^2), root mean square error (RMSE), and sum of squares of errors (SSE). These indicators are necessary to assess the quality of model

fit to experimental data. A high R^2 and low RMSE respectively indicate strong correlation and low prediction error. Integrating these statistical measures into our analysis confirms the relevance of the selected models and ensures the reliability of interpretations of observed drying phenomena.

The quantitative evaluation of model performance is conducted using MATLAB software to provide key statistical parameters. For each model, the software calculates the coefficient of determination (R^2) and adjusted R-squared (Adj- R^2), root mean square error (RMSE), and sum of squares of errors (SSE). These indicators are necessary to assess the quality of model fit to experimental data. A high R^2 and low RMSE respectively indicate strong correlation and low prediction error. Integrating these statistical measures into our analysis confirms the relevance of the selected models and ensures the reliability of interpretations of observed drying phenomena.

IV. RESULTS

- Chemical Screening

The chemical screening of plant bark indicates abundant presence of tannins and alkaloids with methanol solvent, detailed in [Figure 4](#).

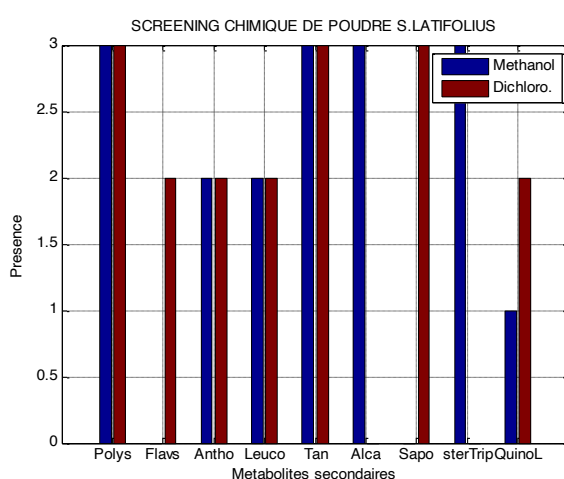


[Figure 4:Presentation of Secondary Metabolites Identified by Screening](#)

(3) : +++ ; (2) :++ ; (1) :+ et (0) :-

In light of the data presented in the table and the histogram above, our analyses reveal a strong presence of polyphenols, tannins, and saponins in the extracts of *Sarcocephalus Latifolius*, obtained with both methanol and dichloromethane. Alkaloids showed a positive reactivity towards the Methanolic extract but no reactivity towards the dichloromethane

extract. Similarly, steroids and triterpenes exhibited favorable reactivity with the Methanolic extract but unfavorable reactivity with the dichloromethane extract. Anthocyanins and leuco-anthocyanins displayed moderate reactivity in both extracts. Flavonoids showed moderate reactivity with the dichloromethane extract, while they exhibited no reactivity with the Methanolic extract. These observations enabled a comprehensive characterization of the chemical composition of *Sarcocephalus Latifolius*, as well as the identification of several secondary metabolites of interest for various applications.

- X-ray Analysis:

The XRF results for the soil (substrate) are in [Figure 6](#), which shows an abundance of silica, followed by alumina in the second position and iron oxide in the third position.

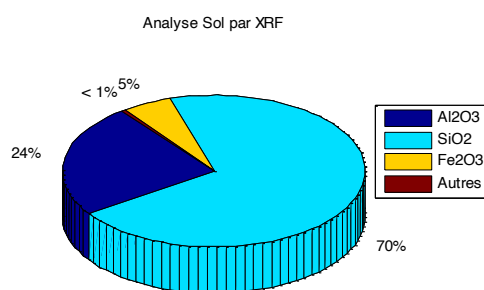


[Figure 6: XRF Results of the soil.](#)

Mineralogical analyses are performed by X-ray diffraction (XRD) using the Bruker D2 Phaser equipment and are presented in Table 1.

[Table 1: XRD Results of *Sarcocephalus Latifolius* root powders.](#)

| SAMPLES | Melanterite <chem>FeSO4.7H2O</chem> | Rozelite <chem>FeSO4.4H2O</chem> | Szomolnokite <chem>FeSO4.H2O</chem> | Gypsum <chem>CaSO4.2H2O</chem> | Bassanite <chem>CaSO4.1/2H2O</chem> | Anhydrite <chem>CaSO4</chem> | Quartz <chem>SiO2</chem> | Jarosite <chem>K+Fe3+(OH)6(SO4)2</chem> | Calcite <chem>CaCO3</chem> | Bianchite <chem>ZnSO4.6H2O</chem> |
|---------|--|-------------------------------------|--|-----------------------------------|--|---------------------------------|-----------------------------|--|-------------------------------|--------------------------------------|
| SPLR | 44.42 | 12.23 | 0 | 0 | 0 | 0.29 | 0 | 0 | 0 | 43.06 |
| SPLB | 3.75 | 9.56 | 0 | 0 | 0 | 0 | 10.89 | 0.1 | 0 | 76.7 |
| SPLD | 14.11 | 3.6 | 13.76 | 0.35 | 0 | 20.27 | 6.71 | 0 | 0.26 | 40.94 |

SPLR: *Sarcocephalus latifolius* root powder. SPLB: *Sarcocephalus latifolius* root powder (burned). SPLD: *Sarcocephalus latifolius* root powder (delipidated)

These data reveal a notable difference in the mineralogical composition of *Sarcocephalus latifolius* barks among the three samples, which may reflect variations in treatment conditions during their preparation. Among the most commonly used plant-derived coagulants are the leaves of *Azadirachta indica* A, Juss, and *Cactus latifolia* L., the fruits of *Dolichos lablab* Linn, and *Phaseolus vulgaris* L., as well as the seeds of *Moringa oleifera* Lam., *Cicer arietinum* L., *Arachis hypogea* L., *Pisum sativum* L., and *Vigna mungo* L. (Hepper) (Koul et al., 2022). Minerals such as melanterite, rozenite, and szomolnokite play an important role in the clarification of raw waters. Melanterite ($\text{FeSO}_4 \cdot 7\text{H}_2\text{O}$) acts as a coagulant agent by promoting the aggregation of suspended particles in raw water, thus facilitating their removal during the filtration process. Similarly, rozenite ($\text{FeSO}_4 \cdot 4\text{H}_2\text{O}$) and szomolnokite ($\text{FeSO}_4 \cdot \text{H}_2\text{O}$) contribute to water clarification (Kanari et al., 2019; Matei & Predescu, 2022). Table 2 illustrates the mass losses of *Sarcocephalus latifolius* bark samples cut into pieces ranging from 0,5 cm to 10 cm in length. The data are expressed as a percentage of the initial sample mass. The columns represent the different sample lengths, ranging from 0,5 cm to 10 cm, while the rows represent the different drying times of the samples. The percentages in the table indicate the amount of mass lost for each sample. The results highlight a general trend of decreasing mass loss with increasing sample length, although fluctuations are observed depending on the sample width.

- Data processing for drying

▪ **Table 2: Mass loss monitoring over time for different bark sizes.**

| Time (Day) | L-0.5 | L-1 | L-2 | L-3 | L-4 | L-5 | L-6 | L-7 | L-8 | L-9 | L-10 |
|------------|-------|-------|-------|-------|-------|-------|-------|-------|-------|-------|-------|
| 0 | 100 | 100 | 100 | 100 | 100 | 100 | 100 | 100 | 100 | 100 | 100 |
| 0.75 | 53.52 | 63.04 | 66.91 | 67.74 | 67.87 | 74.47 | 79.95 | 69.95 | 76.51 | 75.89 | 77.89 |
| 0.875 | 48.03 | 58.85 | 63.25 | 64.35 | 63.82 | 68.90 | 74.78 | 64.68 | 71.47 | 71.74 | 73.43 |
| 1 | 45.55 | 55.87 | 61.08 | 61.71 | 60.61 | 65.59 | 70.84 | 62.37 | 69.01 | 67.94 | 71.31 |
| 1.75 | 35.88 | 47.77 | 52.14 | 50.80 | 47.04 | 54.20 | 58.60 | 48.10 | 55.40 | 55.63 | 60.16 |
| 1.875 | 36.82 | 47.96 | 51.60 | 50.05 | 46.51 | 52.90 | 56.75 | 46.65 | 54.47 | 53.89 | 60.18 |
| 2 | 36.53 | 47.66 | 51.42 | 48.88 | 45.23 | 51.07 | 55.00 | 44.47 | 52.74 | 51.97 | 58.94 |
| 2.791667 | 35.59 | 46.64 | 48.59 | 45.10 | 41.56 | 47.44 | 47.63 | 41.68 | 47.61 | 45.59 | 54.82 |
| 2.875 | 35.70 | 46.95 | 48.66 | 45.46 | 46.71 | 47.31 | 46.94 | 40.40 | 46.96 | 44.94 | 54.36 |
| 2.958333 | 34.37 | 46.53 | 48.39 | 45.08 | 40.84 | 46.93 | 46.12 | 39.81 | 46.27 | 45.11 | 54.06 |
| 3.75 | 35.93 | 46.17 | 47.84 | 44.00 | 39.39 | 46.12 | 42.50 | 38.03 | 42.66 | 41.90 | 51.68 |
| 3.958333 | 34.94 | 46.07 | 47.63 | 43.63 | 38.93 | 45.86 | 41.22 | 37.61 | 41.56 | 40.74 | 50.72 |
| 4.75 | 34.94 | 45.62 | 47.40 | 43.38 | 38.66 | 45.68 | 39.81 | 37.22 | 39.62 | 39.58 | 45.90 |
| 4.875 | 34.94 | 45.77 | 47.14 | 43.15 | 38.53 | 45.61 | 39.65 | 37.10 | 39.19 | 38.87 | 46.10 |

As part of the data processing, specific constants along with statistical fitting parameters are listed in [Table 3](#).

Table 3: Model Constants and Statistical Parameters

| Code | MODEL PARAMETERS & STATISTICAL INDICATORS | PAGE | LOGARITHM | TWO-TERM | VERNA ET AL., | MIDILI | PELEG | LOGISTIC |
|---------|---|----------|-----------|-----------|---------------|----------|----------|-----------|
| Sar-005 | K ₀ , | 0.7579 | 1.642 | 1.508 | 1.501 | 0.8677 | - | 0.8172 |
| | K ₁ , | - | - | -0.02716 | 0.02742 | - | - | - |
| | n | 0.2675 | - | - | - | 0.6793 | - | - |
| | A ₀ | - | 0.6602 | 0.6923 | 0.6887 | 1.002 | 0.5186 | 0.6691 |
| | A ₁ | - | 0.3448 | 0.3117 | - | 0.0589 | 1.378 | 0.3323 |
| | R ² | 0.9463 | 0.9817 | 0.9829 | 0.9828 | 0.9764 | 0.9658 | 0.9727 |
| | SSE | 0.02215 | 0.007555 | 0.007075 | 0.007091 | 0.009736 | 0.0141 | 0.01127 |
| | RMSE | 0.04296 | 0.02621 | 0.0266 | 0.02539 | 0.0312 | 0.03428 | 0.032 |
| Sar-01 | K ₀ , | 0.5782 | 1.627 | - | 0.003849 | 1.59 | 0.6688 | - |
| | K ₁ , | - | - | 1.593 | 0.003913 | - | - | - |
| | n | 0.2358 | - | - | - | 0.5745 | - | - |
| | A ₀ | - | 0.5435 | 0.4515 | 0.5487 | 1.001 | 0.6329 | -0.5503 |
| | A ₁ | - | 0.458 | 0.5497 | - | 0.05682 | 1.664 | 0.4507 |
| | R ² | 0.9722 | 0.9985 | 0.9985 | 0.9985 | 0.994 | 0.9888 | 0.9952 |
| | SSE | 0.007656 | 6 | 0.000417 | 0.000450 | 0.000402 | 0.001661 | 0.003082 |
| | RMSE | 0.02526 | 0.006161 | 0.00633 | 0.006047 | 0.01289 | 0.01603 | 0.01096 |
| Sar-02 | K ₀ , | 0.5039 | 1.343 | 1.367 | - | 0.5873 | - | 0.802 |
| | K ₁ , | - | - | 0.003157 | 0.003128 | - | - | - |
| | n | 0.3001 | - | - | - | 0.6413 | - | - |
| | A ₀ | - | 0.5262 | 0.5206 | 0.5204 | 1.001 | 0.8907 | -0.5389 |
| | A ₁ | - | 0.4738 | 0.4797 | - | 0.05778 | 1.661 | 0.4621 |
| | R ² | 0.9761 | 0.9998 | 0.9998 | 0.9998 | 0.9979 | 0.9933 | 0.998 |
| | SSE | 0.006326 | 6.587e-05 | 5.744e-05 | 5.751e-05 | 0.000568 | 0.001781 | 0.0005268 |
| | RMSE | 0.02296 | 0.002447 | 0.002397 | 0.002286 | 0.001537 | 0.01218 | 0.00692 |

Table 3: Model Constants and Statistical Parameters (continued)

| CODE | MODEL PARAMETERS & STATISTICAL INDICATORS | PAGE | LOGARITHM | TWO-TERM | VERNAA ET AL, | MIDILI | PELEG | LOGISTIC |
|--------|---|----------|-----------|----------|---------------|----------|----------|----------|
| Sar-05 | K0, | 0.4343 | 0.9671 | -0.05055 | 0.7847 | 0.524 | - | 0.478 |
| | K1, | - | - | 0.7971 | 0.05281 | - | - | |
| | n | 0.4456 | - | - | - | 0.8928 | - | |
| | A0 | - | 0.5643 | 0.5643 | 0.6538 | 1.002 | 1.409 | -0.5904 |
| | A1 | - | 0.9952 | 0.6335 | - | 0.07202 | 1.469 | 0.4138 |
| | R ² | 0.9556 | 0.001543 | 0.9973 | 0.9972 | 0.9957 | 0.9811 | 0.9864 |
| | SSE | 0.00141 | 0.01184 | 0.00087 | 0.000887 | 0.00141 | 0.00605 | 0.004331 |
| | RMSE | 0.03437 | 0.5887 | 0.009327 | 0.008984 | 0.01187 | 0.02245 | 0.01984 |
| Sar-06 | K0, | 0.3481 | 0.5887 | 0.4614 | 0.449 | 0.4032 | - | 0.1181 |
| | K1, | - | - | -0.1094 | 0.1208 | - | - | - |
| | n | 0.679 | - | - | - | 1.002 | - | - |
| | A0 | - | 0.6568 | 0.8213 | 0.8309 | 1.002 | 2.311 | -0.7933 |
| | A1 | - | 0.3522 | 0.1825 | - | 0.05329 | 1.128 | 0.2094 |
| | R ² | 0.9823 | 0.9977 | 0.9985 | 0.9984 | 0.9985 | 0.9927 | 0.9934 |
| | SSE | 0.007509 | 0.000969 | 0.00064 | 0.00663 | 0.000658 | 0.003101 | 0.002798 |
| | RMSE | 0.02501 | 0.009386 | 0.00805 | 0.00776 | 0.008083 | 0.01608 | 0.01595 |
| Sar-07 | K0, | 0.4989 | 0.9226 | 0.9212 | 0.9105 | 0.5689 | - | 0.3398 |
| | K1, | - | - | 0.000441 | 0.00202 | - | - | - |
| | n | 0.497 | - | - | - | 0.8424 | - | - |
| | A0 | - | 0.6391 | 0.6398 | 0.6393 | 1.002 | 1.295 | -0.6925 |
| | A1 | 0.01346 | 0.3646 | 0.3638 | - | 0.005381 | 1.277 | 0.31 |
| | R ² | 0.9674 | 0.9904 | 0.9904 | 0.9904 | 0.9885 | 0.9836 | 0.9855 |
| | SSE | 0.01346 | 0.00397 | 0.00397 | 0.003983 | 0.00477 | 0.006782 | 0.006001 |
| | RMSE | 0.03349 | 0.019 | 0.01992 | 0.01903 | 0.02184 | 0.02377 | 0.02336 |

Table 3: Model Constants and Statistical Parameters (continued & end)

| CODE | MODEL PARAMETERS | PAGE | LOGARI THM | TWO-TERM | VERNA ET AL. | MIDL | PELEG | LOGISTI C |
|--------|------------------|----------|------------|----------|--------------|----------|----------|-----------|
| Sar-08 | K ₀ | 0.3849 | 0.6728 | 0.02291 | 0.7194 | 0.4387 | - | 0.1961 |
| | K ₁ | - | - | 0.7317 | -0.02042 | - | - | - |
| | n | 0.6067 | - | - | - | 0.8829 | - | - |
| | A ₀ | - | 0.6288 | 0.4209 | 0.5853 | 1.002 | 1.961 | -0.7257 |
| | A ₁ | - | 0.3722 | 0.582 | - | 0.04663 | 1.215 | 0.277 |
| | R ² | 0.9864 | 0.9987 | 0.9988 | 0.9988 | 0.9979 | 0.9963 | 0.9969 |
| | SSE | 0.005408 | 8 | 0.000511 | 0.000465 | 0.000474 | 0.001455 | 0.001223 |
| | RMSE | 0.02123 | 0.006821 | 0.006823 | 0.006528 | 0.009088 | 0.01101 | 0.01054 |
| Sar-09 | K ₀ | 0.396 | 0.6961 | -0.02932 | 0.629 | 0.4551 | - | 0.2023 |
| | K ₁ | - | - | 0.6375 | 0.03231 | - | - | - |
| | n | 0.6032 | - | - | - | 0.9282 | - | - |
| | A ₀ | - | 0.6365 | -0.02932 | 0.6918 | 1.002 | 1.888 | -0.7281 |
| | A ₁ | - | 0.3679 | 0.6884 | - | 0.05288 | 1.21 | 0.2746 |
| | R ² | 0.9819 | 0.9995 | 0.9993 | 0.9992 | 0.9988 | 0.9942 | 0.001997 |
| | SSE | 0.009403 | 3 | 0.000361 | 0.000300 | 0.000306 | 0.000478 | 0.002376 |
| | RMSE | 0.002484 | 0.005731 | 0.005484 | 0.005279 | 0.006917 | 0.01407 | 0.802 |

We graphically plot smoothing curves over time and deduce the drying characteristics (RMSE, SSE, R², and adj-R²) of our samples using only the Logarithmic model.

In the following lines, we explore the use of the logarithmic model using MATLAB 2020. This model, represented by the equation $f(x) = a \exp(-bx) + c$, with MATLAB 2020, allows us to apply this model to understand and interpret the characteristics and properties of the bark of this plant.

Table 4: Model Constants and Statistical Parameters for the Logarithmic Model

| L(cm) | a | b*e ⁻⁰⁵ | c | RMSE | SSE | R ² | Adj-R ² |
|-------|-------|--------------------|------|--------|-------|----------------|--------------------|
| 0.5 | 65.03 | 2.238 | 35 | 0.7319 | 5.893 | 0.9985 | 0.9982 |
| 1 | 53.35 | 1.883 | 45.8 | 0.6161 | 4.176 | 0.9985 | 0.9982 |
| 2 | 52.62 | 1.554 | 47.4 | 0.2447 | 0.659 | 0.9998 | 0.9997 |
| 3 | 56.91 | 1.331 | 43.1 | 0.2417 | 0.643 | 0.9998 | 0.9998 |
| 4 | 62.51 | 1.184 | 37.9 | 0.6217 | 4.252 | 0.9989 | 0.9987 |
| 5 | 56.61 | 1.111 | 44.2 | 1.12 | 13.79 | 0.9957 | 0.9949 |
| 6 | 65.08 | 0.681 | 35.2 | 0.9386 | 9.691 | 0.9977 | 0.9973 |
| 7 | 64.66 | 1.067 | 35.9 | 0.8902 | 8.718 | 0.9979 | 0.9975 |
| 8 | 62.8 | 0.782 | 37.3 | 0.6679 | 4.907 | 0.9988 | 0.9985 |
| 9 | 63.65 | 0.806 | 36.8 | 0.5731 | 3.613 | 0.9991 | 0.999 |
| 10 | 52.88 | 0.837 | 46.5 | 1.447 | 23.02 | 0.9919 | 0.9904 |

Each row in the table represents a set of data, including corresponding parameters and metrics. It provides a relationship between the sample length and the model coefficients, as well as the overall fit of the model to the observed data. In greater detail, it includes comparisons between different sample lengths, observed trends, and their implications for the studied phenomenon,

Figure 7 presents a kinetic comparison between the 1 cm and 10 cm samples. Both plots illustrate that, for example, at a 50% moisture release rate, the smaller-sized sample reaches this threshold in a considerably shorter period of time.

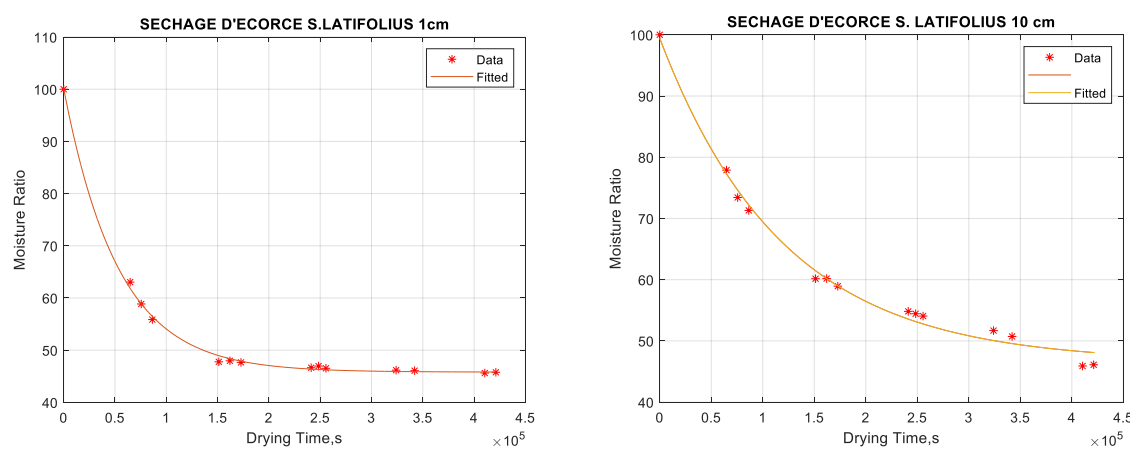


Figure 7: kinetic comparison between the 1 cm and 10 cm samples

Figure 8 provides a visualization of moisture loss over time from different perspectives, Sub-figures (a) and (b) depict this moisture loss in a three-dimensional context, offering a comprehensive view of its evolution. Sub-figure (c) presents a two-dimensional representation for more detailed analysis, while sub-figure (d) specifically shows the drying trend for a 3 cm sample. This visual presentation enhances understanding of the dynamics of moisture loss during the drying process.

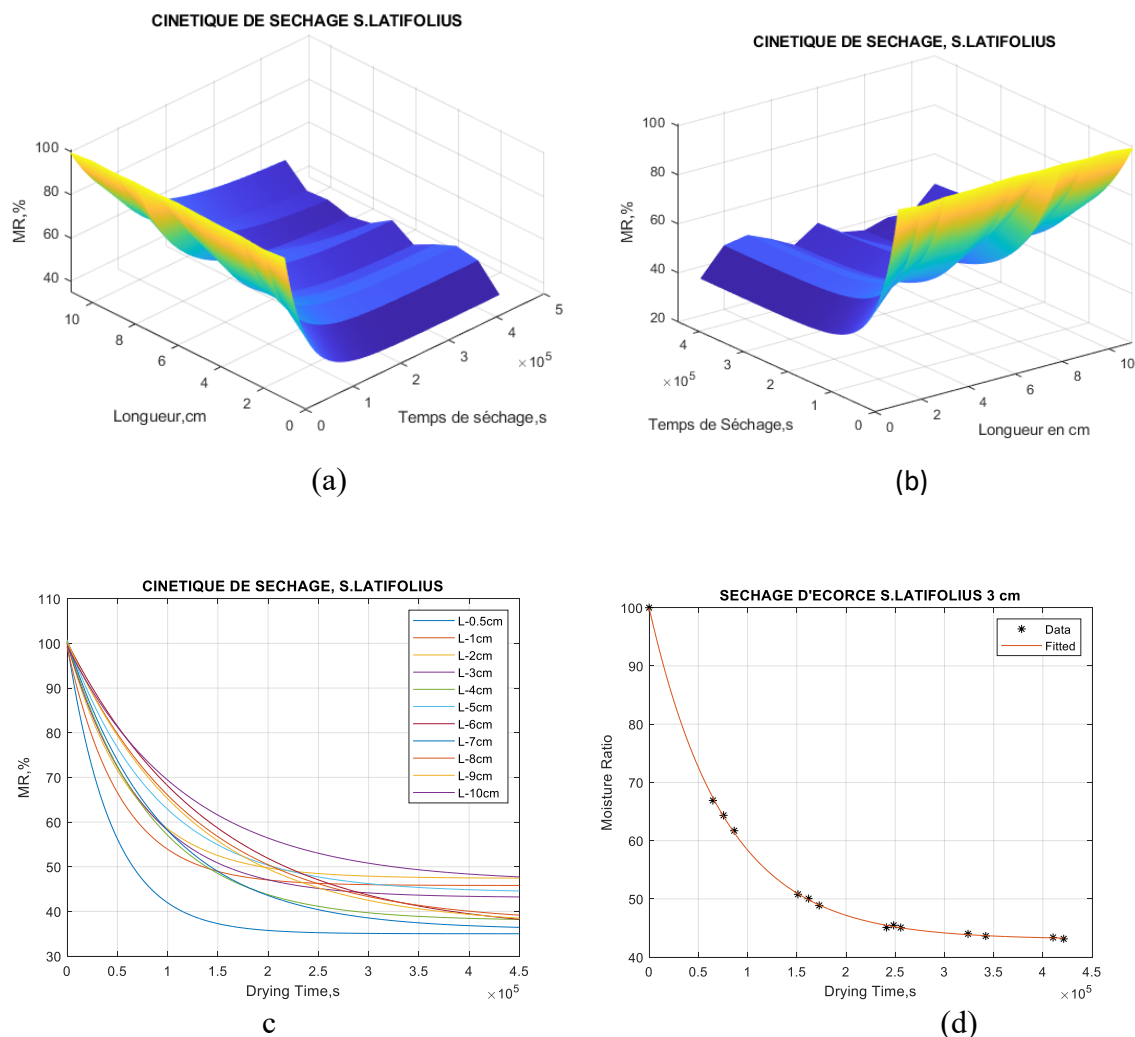


Figure 8: Three-dimensional presentation of moisture loss over drying time (a, b), two-dimensional presentation (c), and drying trend for 3cm sample (d).

[Figure 9](#) illustrates the drying process of 0,5cm dimension bark using the Logarithmic model, while [Figure 10](#) depicts the evolution of the drying rate with the same model.

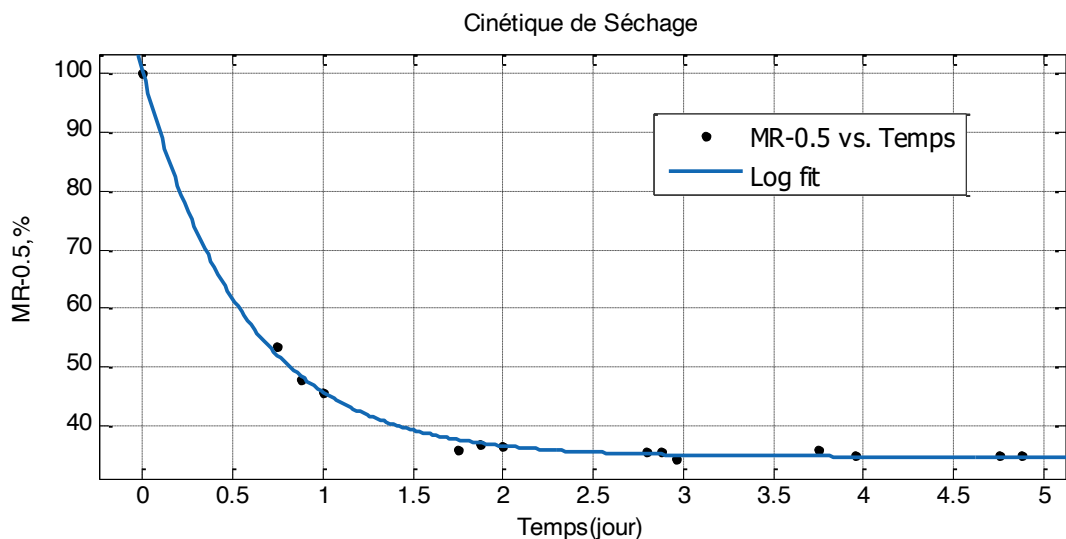


Figure 9 : illustrates the drying process of 0,5cm dimension bark with the Logarithmic model

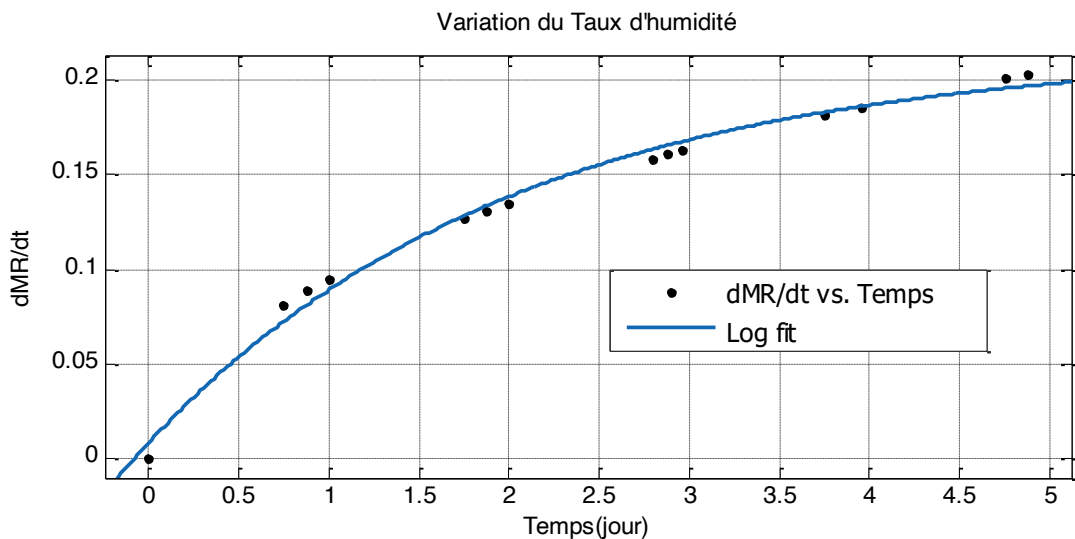


Figure 10 : Depicts the evolution of the drying rate with the same model,

There appears to be a correlation between the duration of bark drying and the drying rate, as indicated by the presented data. Initially, at the beginning of the drying process, the drying rate remains moderate, then it gradually increases with drying time. However, after a certain point, the drying rate seems to reach a plateau, indicating stabilization of the drying process. This phenomenon could result from various factors, such as the presence of residual moisture in the bark or fluctuations in environmental conditions. Further analysis would be necessary to precisely identify the underlying causes of these variations in the drying rate.

V. CONCLUSION

This study on the drying kinetics of *Sarcocephalus latifolius* bark highlights the significant influence of different bark sizes on the efficiency of the desiccation process. Our observations reveal a notable correlation between sample sizes and optimal drying times, indicating a particular sensitivity of smaller fragments to this process.

Furthermore, our results demonstrate the robustness of the logistic and logarithmic models in modeling this drying kinetics, with particularly conclusive validation of the Page model. Moreover, the identification of the significant presence of alkaline sulfates in the bark opens new perspectives for applications, especially in the fields of water purification and prevention of metal corrosion. In summary, this research substantially contributes to the optimization of drying processes and the improvement of the quality of products derived from *Sarcocephalus latifolius*,

BIBLIOGRAPHY

- Badiaga, S., Benkouiten, S., Hajji, H., Raoult, D., Brouqui, P. (2012). Murine typhus in the homeless. Comparative Immunology, Microbiology and Infectious Diseases, 35(1), 39-43. ISSN 0147-9571. [<https://doi.org/10.1016/j.cimid.2011.09.008>] (<https://doi.org/10.1016/j.cimid.2011.09.008>)
- Balogun, M. E., Besong, E. E., Obu, D. C., Obu, M. S. U., Djobissie, S. F. A. (2016). *Nauclea latifolia*: A Medicinal, Economic and Pharmacological Review. International Journal of Plant Research, 6(2), 34-52. <https://doi.org/10.5923/j.plant.20160602.03>
- Boulle, A. (2017). DxTools: processing large data files recorded with the Bruker D8 diffractometer. Journal of Applied Crystallography, 50(3), 967-974. [<https://doi.org/10.1107/S1600576717005192>] (<https://doi.org/10.1107/S1600576717005192>)
- Diarra, N., van't Klooster, C., Togola, A., Diallo, D., Willcox, M., de Jong, J. (2015). Ethnobotanical study of plants used against malaria in Sélingué subdistrict, Mali. Journal of Ethnopharmacology, 166, 352-360. ISSN 0378-8741. [<https://doi.org/10.1016/j.jep.2015.02.054>] (<https://doi.org/10.1016/j.jep.2015.02.054>)
- El Mtiai, W. (2023). Les formes d'utilisation des plantes médicinales. Thèse de Doctorat, UNIVERSITE MOHAMMED V DE RABAT, p166, N°: 047. <http://toubkal.imist.ma/handle/123456789/19333>
- Ishimwe, E. (2008). EFFETS DE L'INFUSE DES RACINES ENTIERES DE *Nauclea latifolia* Sm. SUR LES PERFORMANCES DE REPRODUCTION: Etude expérimentale chez le Rat. Thèse de doctorat, UNIVERSITE CHEIKH ANTA DIOP DE DAKAR, p97, N° 29.
- Kanteh, S. M., Norman, J. E. (2015). Diversity of plants with pesticidal and medicinal properties in southern Sierra Leone. Biological Agriculture & Horticulture, 31(1), 18-27. [<https://doi.org/10.1080/01448765.2014.945621>] (<https://doi.org/10.1080/01448765.2014.945621>)
- Kuete, V., Seukep, A. J. (2023). Chapter Eight - Phytochemistry and antibacterial potential of the genus *Nauclea*. Advances in Botanical Research, 107, 239-273. ISSN 0065-2296, ISBN 9780443188848.

- [<https://doi.org/10.1016/bs.abr.2022.08.018>] [<https://doi.org/10.1016/bs.abr.2022.08.018>]
- Lalit, R., Verma, R. A., Bucklin, J. B., Endan, F. T., Wratten, (1985). Transactions of the ASAE, 28(1): 0296-0301. [<https://doi.org/10.13031/2013.32245>]
 - Masters, E.T. (2023). Medicinal plants of the upper Aswa River catchment of northern Uganda - a cultural crossroads. J Ethnobiology Ethnomedicine, 19, 48. [<https://doi.org/10.1186/s13002-023-00620-5>] [<https://doi.org/10.1186/s13002-023-00620-5>]
 - Rodrigo Leite Moura, Rossana Maria Feitosa de Figueirêdo, Alexandre José de Melo Queiroz, Francislaine Suelia dos Santos, Antônio Gilson Barbosa de Lima, Pedro Francisco do Rego Junior, Josivanda Palmeira Gomes, Wilton Pereira da Silva, Yaroslávia Ferreira Paiva, Henrique Valentim Moura, Eugênia Telis de Vilela Silva, Caciana Cavalcanti, Mailson Gonçalves Gregório. (2023). Smelling Peppers and Pout Submitted to Convective Drying: Mathematical Modeling, Thermodynamic Properties and Proximal Composition. Foods, 12(11), 2106. [<https://doi.org/10.3390/foods12112106>] [<https://doi.org/10.3390/foods12112106>]
 - Nadia, B. M. A., Emmanuel, A. M., Ernest, Z. N. (2021). Phytochemical Study, Acute Toxicity, and Fertility Potential Effect of *Sarcocephalus latifolius* (Smith) on the Histology of Wistar Rats Testicles. European Journal of Medicinal Plants, 32(2), 62-69. [<https://doi.org/10.9734/ejmp/2021/v32i230373>] [<https://doi.org/10.9734/ejmp/2021/v32i230373>]
 - Nurudeen, Q. O., Salimon, S. S., Falana, M. B., Yakubu, M. T., Akanji, M. A. (2022). Ethnopharmacological Survey of Plants Used for the Treatment of Female Sexual Dysfunction and Infertility in Ilorin, Nigeria. Traditional and Integrative Medicine. [<https://doi.org/10.18502/tim.v7i1.9068>] [<https://doi.org/10.18502/tim.v7i1.9068>]
 - Okhale, S. E., Okoli, C. P., Imoisi, C., Aliyu, A., Kazeem, T., Ogweke, V. (2023). Phytochemical and synergistic antimicrobial effects of *Morinda lucida*, *Anogeissus leiocarpus* and *Sarcocephalus latifolius* leaf extract. Life Science Journal, 20(4) <https://doi.org/10.3923/asb.2024.425.434>
 - Oise, I. E., Adesina, A. B., Oluwasegun, A. A. (2014). Comparative phytochemical, cytotoxic and growth inhibitory effects of the leaf and root barks of *Sarcocephalus latifolius* (JE Smith) EA Bruce (Rubiaceae). [<http://dx.doi.org/10.12692/ijb/4.4.162-169>] [<http://dx.doi.org/10.12692/ijb/4.4.162-169>]

- Page, G. E. (1949). Factors Influencing the Maximum Rate of Air Drying Shelled Corn in Thin-Layers. Master's Thesis, Purdue University, West Lafayette, Indiana. <https://api.semanticscholar.org/CorpusID:137309822>
- Paiva, Y. F., Figueirêdo, R. M. F., Queiroz, A. J. M., Ferreira, J. P. L., Santos, F. S., Reis, C. G., Amadeu, L. T. S., Lima, A. G. B., Gomes, J. P., Silva, W. P. (2023). Tropical Red Fruit Blends: The Effect of Combination of Additives on Foaming, Drying and Thermodynamic Properties. Processes, 11, 888. [https://doi.org/10.3390/pr11030888](<https://doi.org/10.3390/pr11030888>)
- Plassart, L. (2015). *Sarcocephalus latifolius* (Sm,) Bruce: études botaniques, chimique et pharmacologique. Thèse, France, 151p. dumas-01158031
- **Sibiry Albert KABORÉ.** (2015). Évaluation des services écosystémiques de *Crateva adansonii* D. C., *Sarcocephalus latifolius* (Smith) Bruce et *Burkea africana* Hook dans la région du Sud-Ouest du Burkina Faso. Thèse, Burkina Faso, UNIVERSITE POLYTECHNIQUE DE BOBO-DIOULASSO, 153p. <https://doi.org/10.4314/ijbcs.v9i3.5>
- Togola, I., Konaré, M. A., Dembele, H., Samake, S., Diarra, N. (2023). Plants Used in the Traditional Treatment of Female Infertility in Kita, Mali. Annual Research & Review in Biology, 13-24. [https://doi.org/10.9734/arrb/2023/v38i1230619](<https://doi.org/10.9734/arrb/2023/v38i1230619>)
- Traoré, L., Yaro, V. S. O., Soudré, A., Ouédraogo-Koné, S., Ouédraogo, D., Yougbaré, B., Zoma, B. L., Hien, M., Guissou, M.-L., Traoré, A., Mészáros, G., Wurzinger, M., Burger, P., Okeyo, A. M., Thiombiano, A., Sölkner, J. (2020). Indigenous knowledge of veterinary medicinal plant use in cattle treatment in southwestern Burkina Faso (West Africa). South African Journal of Botany, 128, 189-199. ISSN 0254-6299. [https://doi.org/10.1016/j.sajb.2019.09.015]<https://doi.org/10.1016/j.sajb.2019.09.015>